

ENSO signal in continental temperature and precipitation records

R. S. Bradley*, H. F. Diaz†, G. N. Kiladis‡
& J. K. Eischeid‡

* University of Massachusetts, Amherst, Massachusetts 01003, USA

† National Oceanic and Atmospheric Administration, Environmental Research Laboratory, Boulder, Colorado 80303, USA

‡ Cooperative Institute for Research in Environmental Sciences, University of Colorado, Boulder, Colorado 80309, USA

Warm events in the tropical Pacific Ocean, associated with one extreme of the Southern Oscillation (generally known as El Niño–Southern Oscillation or ENSO events) are now known to be of global significance in perturbing the general circulation of the atmosphere^{1–8}. It is also apparent that episodes of enhanced cold-water upwelling ('cold events') have an impact on large-scale atmospheric circulation patterns^{9–11}. Here we examine the effect of warm and cold events on short-term fluctuations of continental surface air temperature and precipitation throughout the Northern Hemisphere using a newly compiled set of high-quality temperature and precipitation data^{12–13}. The data were in the form of gridded anomalies from a 1951–70 reference mean for temperature and a 1921–60 reference mean for precipitation^{13–14}.

A commonly used index of the Southern Oscillation is the normalized sea-level pressure difference between Tahiti and Darwin^{15,17}. With this index (SOI), large negative values correspond to warm events and large positive values to cold events. A five-month running mean of the index is shown in Fig. 1, together with a corresponding five-month running mean of average monthly temperature anomalies for the land areas of the latitude zone 0–25° N. This area includes sub-Saharan Africa, southern India, south-east Asia, central America and northern South America. It is clear that the temperature series exhibits periods of persistent positive anomalies separated abruptly from periods of persistent negative anomalies. Furthermore, the positive temperature anomalies correspond to times when the SOI is negative and vice versa. This is consistent with other studies (based on more limited data) which have reported evidence of a strong correlation between equatorial Pacific sea surface temperature (SST) and tropical tropospheric mean temperature (TTT), with SST leading TTT by about 6 months^{3,18–22}. Note also that the relative absence of periods of positive SOI in the past 10 years corresponds to a period of persistently high temperatures. A regression of monthly SOI and monthly temperature anomalies over the period 1910–1980 shows a strong negative relationship ($r = -0.41$, $p = 0.01$), with maximum correlation when the SOI leads by five months.

To examine the time-dependent relationship between warm and cold events and continental surface temperatures at different latitudes, a superposed epoch analysis was performed²³. The selection of key dates was based on the Tahiti–Darwin pressure series and a separate index composed of sea surface temperature anomalies averaged from 4° N–4° S, 160° W to the South American coast²⁴. Based on these indices and previous studies^{10,24–26}, the starting year (year 0) of 23 warm events and 20 cold events was identified in the period 1881–1980 (see Fig. 2 legend). The SOI was then averaged by month, from January of the year preceding each event (year -1) to the December of the year following it (year +1). This produced a composite SOI time series for both ENSO extremes (Fig. 2). The SOI changes sign, on average, in April of the event year. Thus, April of each year shown in the legend of Fig. 2 was selected as the key month for superposed epoch analysis of temperature change over continental regions. Temperature anomalies were standardized (to accommodate differences in variance from summer to winter months) by dividing each monthly anomaly by the standard

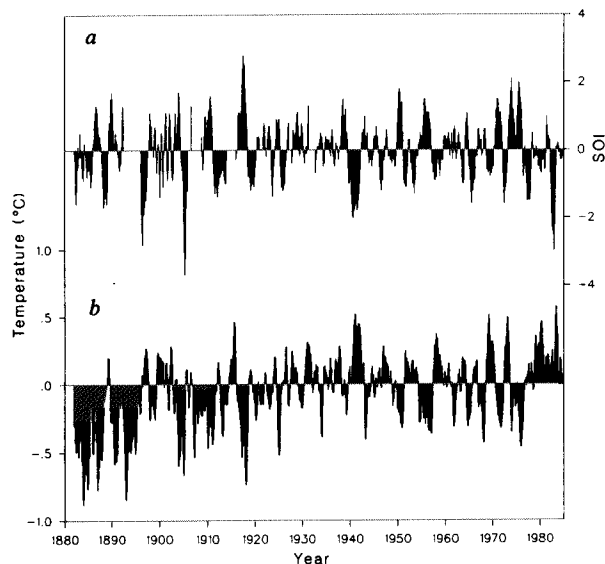


Fig. 1 *a*, Southern Oscillation index based on normalized series of Tahiti–Darwin sea-level pressure (both station sets normalized). Negative values correspond to warm (ENSO) events, the extremes of which are El Niño events; *b*, average temperature anomaly (with reference to 1951–1970) over continental areas 0–25° N based on a gridded data set¹³. Values are five-month running means.

deviation of the respective month in the period 1881–1980. Because we are interested in the effects of ENSO events on prevailing temperatures at various times during each event, the superposed epoch analysis was carried out with respect to the mean of the 36 months preceding each warm and cold event. In this way the effects of warm and cold events during generally colder than average periods are comparable with their effects during generally warmer than average periods. Zonally averaged anomalies for each 5° latitude band from 5° N to 70° N were computed for the 36 months before and 36 months following each warm event. As a check, the same procedure was performed on two separate sets of both warm and cold event years; namely those before 1925 and after 1925. Similar results were obtained for each of these independent runs, confirming the reliability of the signals.

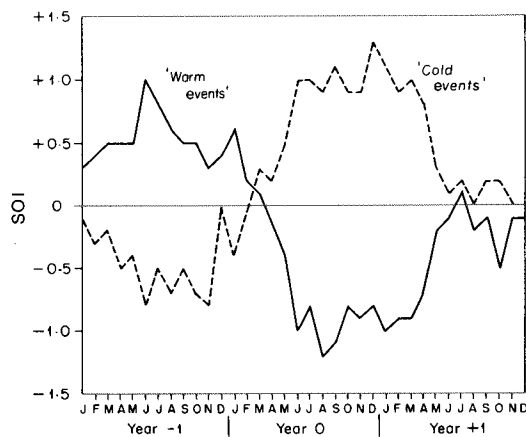


Fig. 2 Composite SOI sequence derived by averaging monthly values centred on the cold event and warm event years. The warm event years are: 1884, 1888, 1891, 1896, 1899, 1902, 1904, 1911, 1913, 1918, 1923, 1925, 1930, 1932, 1939, 1951, 1953, 1957, 1963, 1965, 1969, 1972, 1976. The cold event years are: 1886, 1889, 1892, 1898, 1903, 1906, 1908, 1916, 1920, 1924, 1928, 1931, 1938, 1942, 1949, 1954, 1964, 1970, 1973, 1975.

Fig. 3 Superposed epoch analysis of temperature anomalies over continental areas for warm (solid) and cold (dashed) ENSO events. Temperature anomalies (from 1951 to 1970 mean) normalized by standard deviation of respective month for period 1881–1980. Anomalies expressed as departures from 36-month average before April of Year 0. Key years are shown in Fig. 2 legend. Dashed horizontal lines show levels of significance at the 5% level.

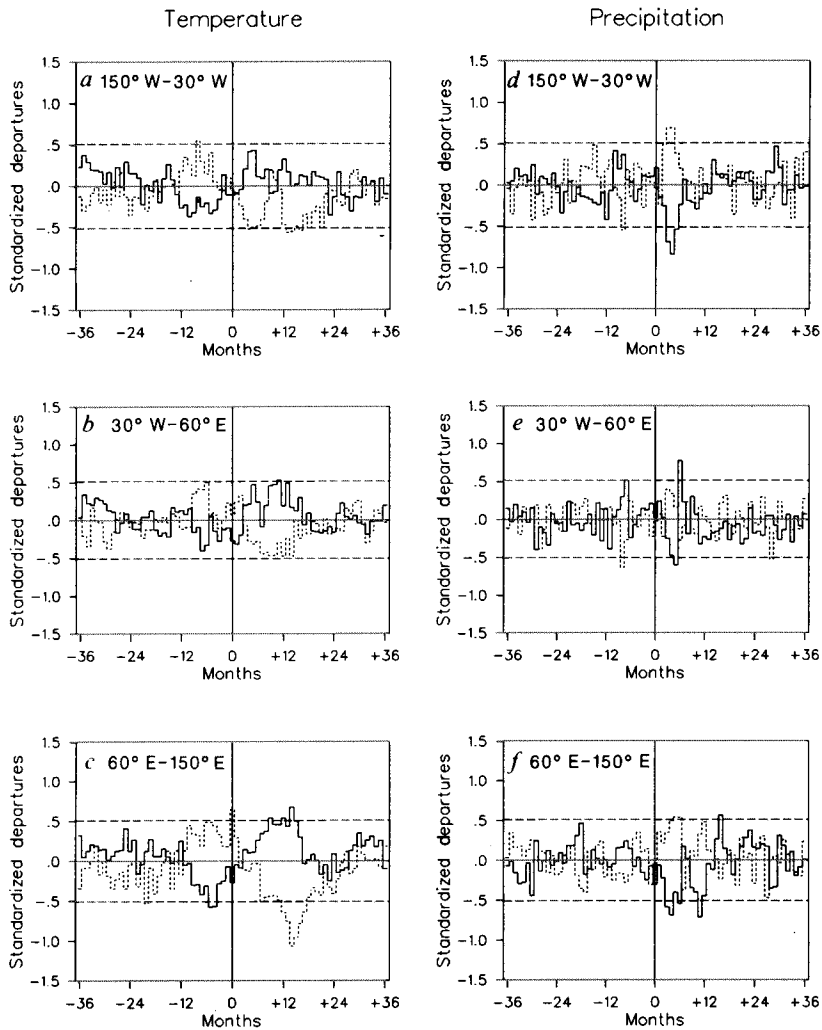
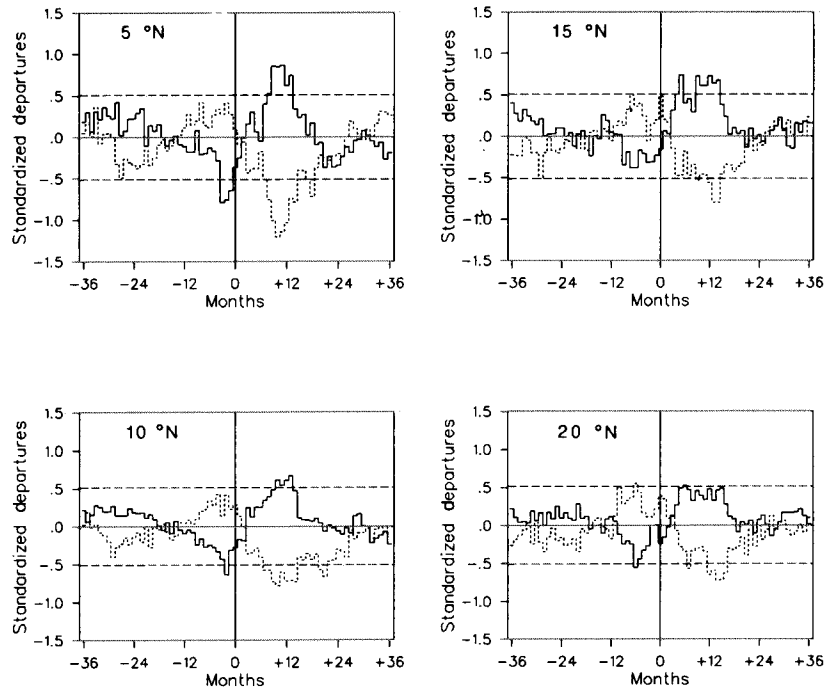


Fig. 4 As in Fig. 3, except for regional averages (0° – 30° N over the indicated longitudes).

To assess the statistical significance of the anomalies a Monte Carlo approach was used. Four-hundred simulations of 20 randomly selected dates within the interval 1881–1980 were used to determine appropriate confidence levels. In general, the 5% significance level falls close to the $\pm 0.5\sigma$ composite mean level.

Figure 3 shows the composite warm and cold event time series of zonally-averaged temperature for the four latitude bands with the strongest signals (5° to 20° N). For warm events, approximately 12 months before April of year 0 an abrupt decline in temperature occurs in the tropics, reaching levels significantly below average from around July (year -1) to March (year 0) (Fig. 3a–d, solid curve). Temperatures then rise rapidly, reaching levels significantly above average from August through July of the following year, after which temperatures return to near normal. Maximum negative anomalies occur, on average, in the autumn and winter of year -1 and maximum positive anomalies in the winter and spring of year $+1$ (two to three months after the SOI composite minimum). However the switch from well below to well above average temperatures occurs very rapidly, in the course of only 3–4 months. The results of the same procedure applied to cold events are shown as the dashed curves in Fig. 3a–d. In the tropics the temperature anomalies clearly follow the opposite course, being well above average before April of year 0 and falling abruptly thereafter. Minimum temperatures occur in spring and early summer of year $+1$, 12 months or so after the SOI composite maximum. The composite responses to warm and cold events have a correlation coefficient of -0.80 ($p=0.01$). This pattern of opposite trends is, in part, related to the fact that cold and warm events often follow each other closely in time (see Fig. 2 legend) and hence the superposed epoch analyses overlap in many instances. Nevertheless, the

data clearly show that the change from one phase of the Southern Oscillation to another is reflected in relatively large shifts in the temperature anomaly pattern throughout the Northern Hemisphere tropics.

It has been shown that climate anomalies associated with the evolution of ENSO vary spatially as well as temporally^{27–30}. Therefore, we repeated the analysis, this time focusing on selected continental regions from 0 – 30° N (Fig. 4). The three tropical regions selected cover the Americas (150° W– 30° W), North Africa (30° W– 60° E) and southern Asia (60° E– 150° E). As in Fig. 3, all regions show above normal temperatures at the end of year 0 of warm events and below normal temperatures during cold events, with the opposite signal during year -1 . This signal is strongest and occurs latest in the Asian sector (Fig. 4c), while in the American sector, the signal is stronger during cold rather than warm events (Fig. 4). Thus, the signals of Figs 3 and 4 are not due to any particular sector, but appear to occur globally.

The superposed epoch analysis was repeated to determine the time variation of large-scale precipitation anomalies associated with ENSO events (Figs 4d–f and 5). During warm events, precipitation over the zonally averaged continental areas of the Northern Hemisphere tropics tends to be low, with two distinct anomalies (Fig. 5). The first occurs during the northern summer monsoon season, and reflects the tendency for below normal precipitation to occur over southern Asia^{25–29,31,32} and the Sahel region of Africa³⁰. This is clearly illustrated in the regional graphs (Fig. 4d–f). The source of the second minimum around March of year $+1$ is primarily from the tropical Asian sector (Fig. 4f), although the signal is also evident in the other two sectors. The changes during cold events are generally the reverse of those during warm events. The positive (negative) precipita-

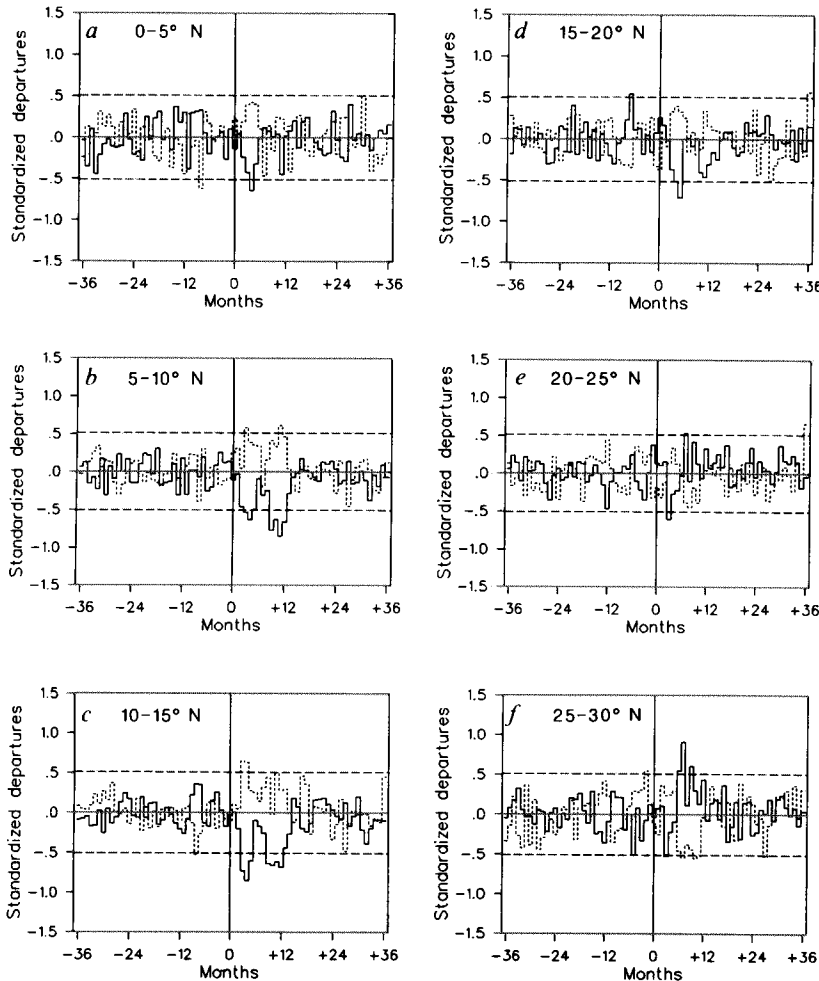


Fig. 5 As in Fig. 3, except for zonal precipitation anomalies. Precipitation anomalies (from 1921 to 1960 mean) normalised by standard deviation of respective month for period 1881–1980.

tion anomaly north of 20° N occurs in the winter months during year +1 of warm (cold) events. It is due principally to an increase (decrease) in precipitation over the southeastern United States (Fig. 4e) during warm (cold) events. Anomalies over the African continent exhibit the least coherence and signal strength of the three regions.

As these regional data show, there is considerable variability across longitudes not only with regard to the amplitude of the anomalies, but also, in some instances with regard to the sign⁵. Nevertheless, it is clear that ENSO events have a powerful influence on large-scale temperature and precipitation patterns in the Northern Hemisphere. ENSO-related anomalies in the

Southern Hemisphere are also significant and have been detected far from the original source of forcing^{5,10}.

The large spatial scale and long-lived nature of the surface temperature and precipitation anomalies, together with the fact that the climatic response has the opposite tendency during ENSO extremes make these findings of some practical importance. The swings in temperature and precipitation associated with ENSO contribute a large fraction of the interannual variability in the tropics and portions of the extratropics.

This work was funded by the Carbon Dioxide Research Division, US Department of Energy.

Received 31 October 1986; accepted 23 March 1987.

1. Troup, A. J. *Q. Jl R. met. Soc.* **91**, 490-506 (1965).
2. Bjerknes, J. *Month. Weath. Rev.* **97**, 163-172 (1969).
3. Horel, J. D. & Wallace, J. M. *Month. Weath. Rev.* **109**, 813-829 (1981).
4. van Loon, H. & Rogers, J. C. *Month. Weath. Rev.* **109**, 1163-1168 (1981).
5. van Loon, H. & Madden, R. A. *Month. Weath. Rev.* **109**, 1150-1162 (1981).
6. Rasmusson, E. M. & Carpenter, T. H. *Month. Weath. Rev.* **109**, 1150-1162 (1982).
7. Yarnal, B. *Progr. Phys. Geogr.* **9**, 315-352 (1985).
8. Kiladis, G. N. & Diaz, H. F. *Month. Weath. Rev.* **114**, 1035-1047 (1986).
9. Yarnal, B. and Diaz, H. F. *J. Climat.* **6**, 197-219 (1986).
10. van Loon, H. & Shea, D. J. *Month. Weath. Rev.* **113**, 2063-2074 (1985).
11. Philander, S. G. H. *J. Atmos. Sci.* **42**, 2652-2662 (1985).
12. Bradley, R. S., Kelly, P. M., Jones, P. D., Goodess, C. M. & Diaz, H. F. *A Climatic Data Bank for Northern Hemisphere Land Areas 1851-1980*, Tech. Rep. 017 (US Dept. of Energy, Washington, DC, 1985).
13. Jones, P. D. *et al. J. Clim. appl. Met.* **25**, 161-179 (1986).
14. Bradley, R. S. *et al. Science* (in the press).
15. Chen, W. Y. *Mon. Weath. Rev.* **110**, 800-807 (1982).
16. Parker, D. E. *Met. Mag.* **112**, 184-188 (1983).
17. Jones, P. D. & Ropelewski, C. F. *Month. Weath. Rev.* (in the press).
18. Newell, R. E. & Weare, B. C. *Nature* **262**, 40-41 (1976).
19. Angell, J. K. *Month. Weath. Rev.* **109**, 230-243 (1981).
20. Angell, J. K. & Korshover, J. *Month. Weath. Rev.* **111**, 901-921 (1983).
21. Pan, Y. H. & Oort, A. H. *Month. Weath. Rev.* **111**, 1244-1258 (1983).
22. Parker, D. E. *J. Climat.* **5**, 273-282 (1985).
23. Conrad, V. & Pollock, L. W. *Methods in Climatology* (Harvard University Press, Cambridge, Massachusetts, 1950).
24. Fu, C., Diaz, H. F. & Fletcher, J. O. *Month. Weath. Rev.* **114**, 1716-1738 (1986).
25. Quinn, W. H., Zopf, D. O., Short, K. S. & Kuo Yang, R. T. W. *Fish. Bull.* **76**, 663-678 (1978).
26. Wright, P. B. *An Index of the Southern Oscillation* (Climatic Research Unit Publication CRU RP4, Univ. of East Anglia, Norwich, UK, 1975).
27. Rasmusson, E. M. & Wallace, J. M. *Science* **222**, 1195-1202 (1983).
28. Meehl, G. A. *Month. Weath. Rev.* (in the press).
29. Berlage, H. P. *Mededelingen en Verhandelingen* No. 69 (Koninklijk Netherlands Meteorologische Instituut, Staatsdrukkerij, S'Gravenhage, Netherlands, 1957).
30. Ropelewski, C. F. & Halpert, M. S. *Month. Weath. Rev.* (in the press).
31. Bhalme, H. N. & Jadhav, S. K. *J. Climat.* **4**, 509-520 (1984).
32. Parthasarathy, B. & Part, G. B. *J. Climat.* **5**, 369-378 (1985).